Measuring drug effect on cell cycle profile using the Cellometer Vision image cytometer.

Introduction

Cell cycle analysis is a commonly used assay in both clinical diagnosis and biomedical research. This analysis distinguishes cells in different phases of cell cycle and is often used to determine cellular response to drugs and biological stimulations [1, 2]. Because this assay is based on measuring the DNA content in a cell population, it can also be used to analyze DNA fragmentation during apoptosis, requiring multicolor fluorescent staining of biomarkers and DNA [3].

Recently, a small desktop imaging cytometry system (Cellometer Vision) has been developed for automated cell concentration and viability measurement using brightfield (BR) and fluorescent (FL) imaging methods [4]. The system can perform rapid cell enumeration using disposable counting slides. The software utilizes a novel counting algorithm for accurate and consistent measurement of cell concentration and viability on a variety of cell types [5]. By developing fluorescent-based cell cycle assays, the Cellometer imaging cytometry can provide a quick, simple, and inexpensive alternative for biomedical research, which may be beneficial for smaller research laboratories and clinics.

In this work, we demonstrate new applications of the Cellometer Vision for fluorescencebased cell population analysis as an alternative for flow cytometry. Cell cycle analysis was performed by inducing specific arrest in G_0/G_1, S, and G_2/M phase of Jurkat cell population with aphidicolin, etoposide, and nocodazole, respectively [6-8]. The results were compared between the image-based and conventional flow cytometry methods.

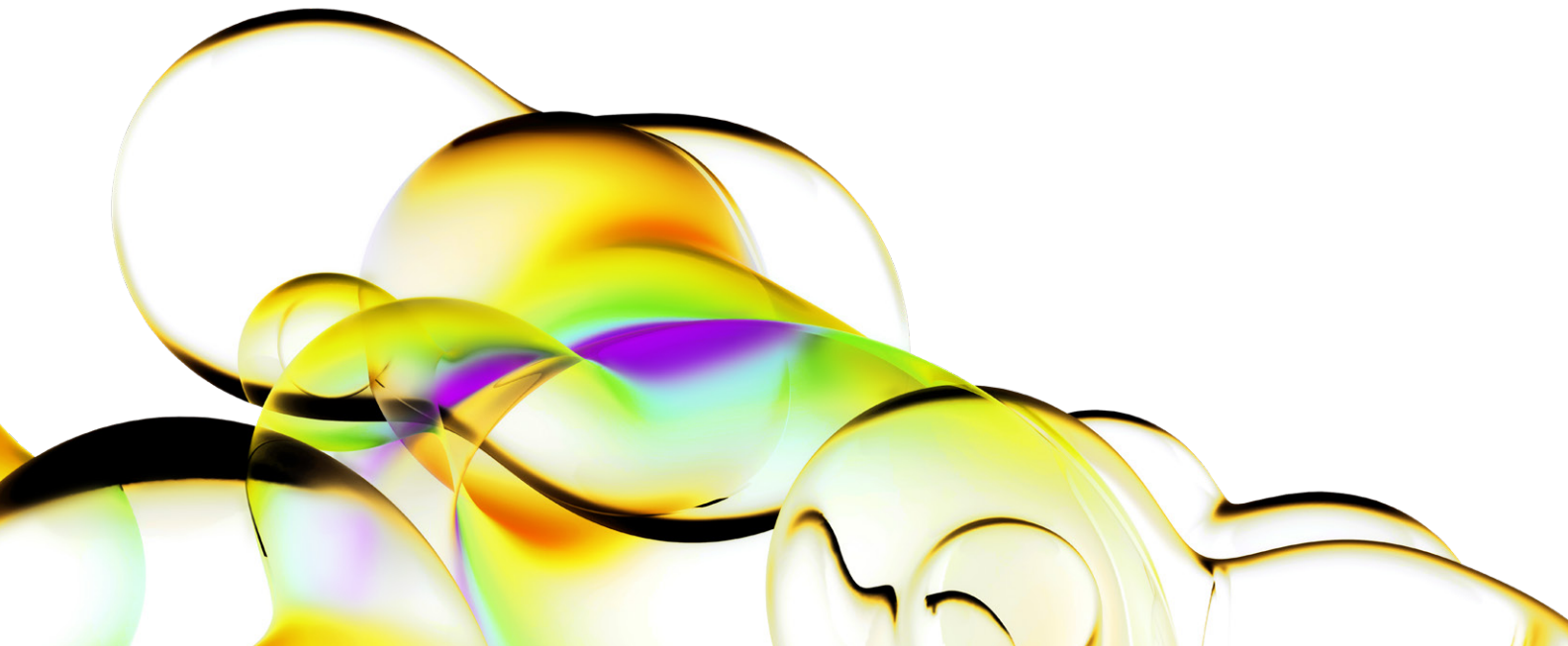

Materials and methods

Cellometer Vision and disposable counting chamber

The Cellometer Vision utilizes one brightfield and two fluorescent channels to perform image-based cytometric analysis. Brightfield imaging used a broadband white light-emitting diode (LED) and fluorescence imaging used three different monochromatic LEDs (470, 527, and 630 nM) as the excitation light sources. Each monochromatic excitation was paired with a specific excitation (nM)/emission (nM) filter set (475/ 525, 475/595, 527/595, and 630/695) with a bandwidth of approximately 40 nM.

Cellometer systems were designed to specifically analyze Revvity's disposable counting chamber, which holds precisely 20 µL of sample. Four separate areas were imaged and analyzed sequentially by the system, where the target cells were identified and counted by the software. In general, combined image acquisition and cell counting time was approximately 30 seconds.

The Cellometer software used a proprietary algorithm to analyze the captured brightfield and fluorescent images. Parameters such as cell shape circularity and size were gated to count specific population of cells from the brightfield images. Aggregation of cells was included in the total cell count by the use of declustering function, which could distinguish and count individual cells in the cluster. Fluorescent intensity within individually counted cells was measured with sample-dependent fluorescent threshold, based on which a histogram plot was generated to show distribution of fluorescent intensity in the population. Counting and fluorescence measurements were directly exported to FCS Express™ (De Novo Software) for flexible graph generation. Exported data file contained the number, size, and fluorescence intensity of individually counted cells.

Cell preparation for cell cycle analysis

The Jurkat cell line (TIB-152) was cultured in RPMI medium with 10% fetal bovine serum. The cell culture was maintained in an incubator at 37 °C with 5% CO_2.

Three cell-cycle-arresting reagents, nocodazole, etoposide, and aphidicolin were used to induce arrest at different cell cycle phases. Jurkat cells were harvested from the culture flasks and centrifuged. The pellet was resuspended in fresh media and separated into 10 different flasks containing nocodazole (0.1, 0.02, and 0.004 µg/mL), etoposide (3, 0.6, and 0.12 µM), aphidicolin (30, 6, and 1.2 µg/mL), and a control with only media. The Jurkat cells were then cultured for 24 h. At the end of the culture, the Jurkat cells were centrifuged and the pellet was resuspended in phosphate buffered saline (PBS). The cells were fixed with ethanol and incubated on ice. The cells were then centrifuged and the pellet was resuspended in propidium iodide (PI) solution containing PI, RNase A, and Triton X-100. The Jurkat cells were incubated for 40 min at 37 °C before performing flow and imaging cytometry analysis.

Flow cytometry analysis

Fluorescence intensity data were acquired from a FACS- Calibur flow cytometer. A 488 nM and a 635 nM excitation laser and PE emission were used for cell cycle analysis. The measured results were analyzed using the FlowJo software and compared with that of Cellometer imaging cytometry.

Results

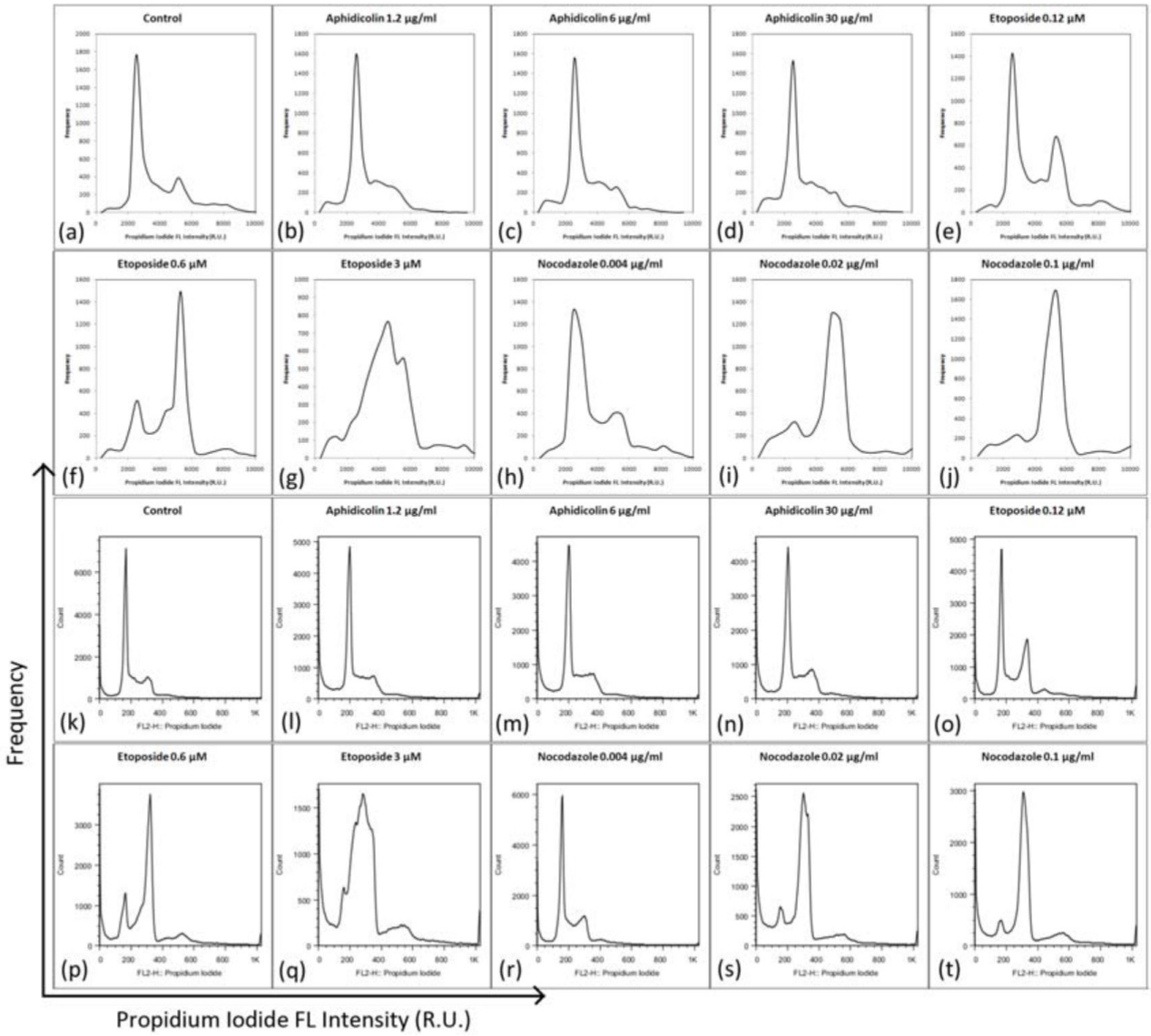

Figure 1: Cell cycle analysis of Jurkat cells.

Cell cycle arrest of Jurkat cells was induced with aphidicolin, etoposide, and nocodazole, respectively, at the indicated dose. Cell cycle arrest was determined by DNA content analysis using PI staining and analyzed by both Cellometer (Figs. 1a–1j) and flow cytometry (Figs. 1k–1t).

For aphidicolin-induced arrest, the percentage of cells at G0/G1 and S phase increased by 2–3% in a dose-dependent manner.

Cells were arrested at S and G2/M phase after etoposide and nocodazole treatment and the percentage of cell-cycle arrested cells also showed a dose-dependent increase (~10 and 35%, respectively). Experimental variation ranged from 0 to 6%.

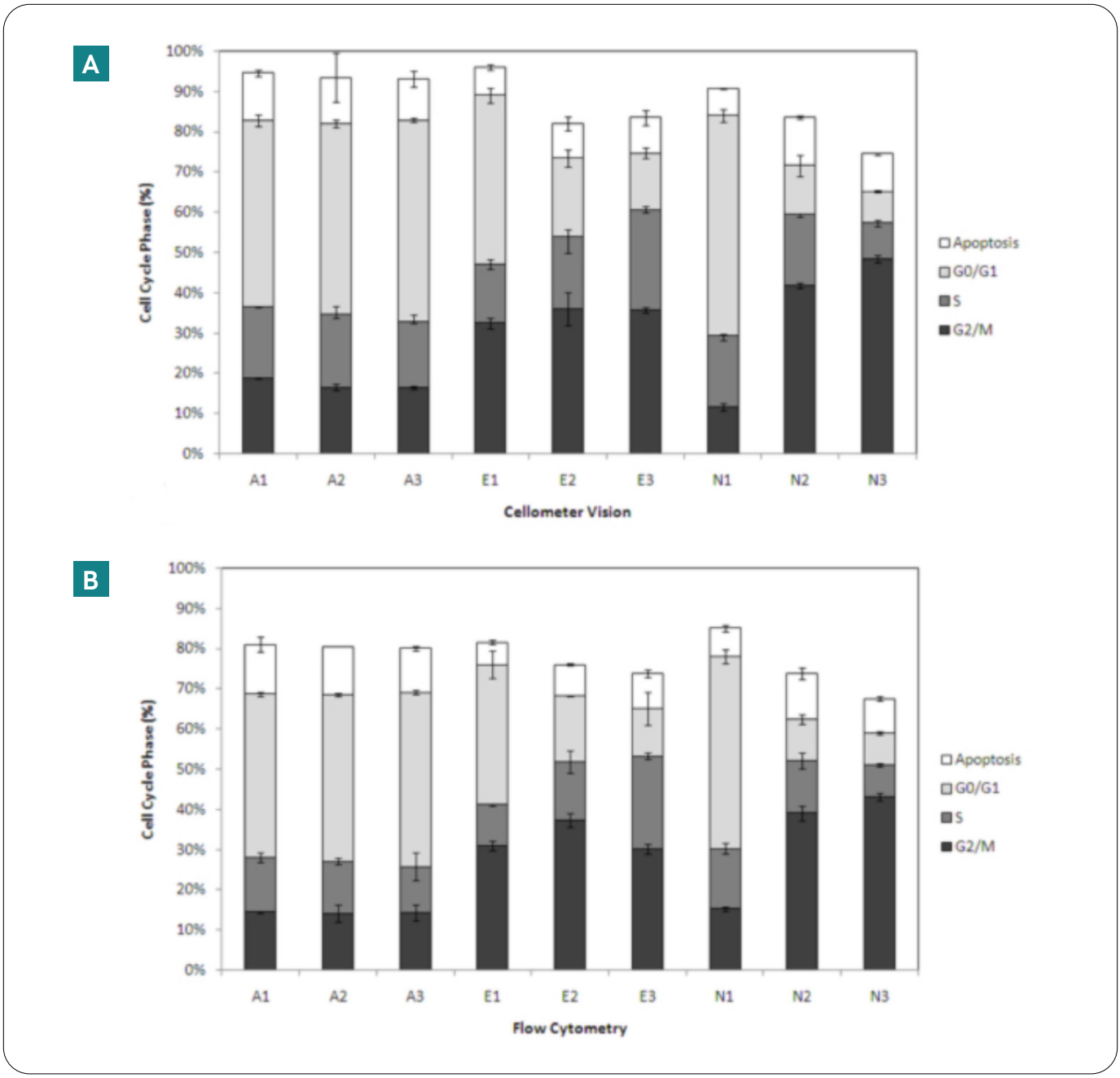

Figure 2: Plot of cell cycle phase percentages.

Cell cycle arrest was induced by aphidicolin, etoposide, and nocodazole in G0/G1, S, and G2/M phase, respectively. The drug-induced Jurkat cells were measured with (A) Cellometer (n = 4) and (B) flow cytometry (n = 2).

Aphidicolin-treated samples showed an increase of ~2-3% in the G0/G1 phase.

Etoposide-treated samples showed an increase of ~10% in the S phase.

Nocodazole-treated samples showed an increase of ~35% in the G2/M phase, which were consistent with flow cytometry results.

The cell cycle data were comparable between the Cellometer image cytometry and flow cytometry with ± 5% difference.

Conclusions

- The ability to rapidly and cost-effectively perform cell population analysis may improve research efficiency, especially where a flow or laser scanning cytometer is not available or in situations where a rapid analysis of data is critical.
- Cellometer Vision performed the cell cycle assay outlined here and achieved results consistent with those of the conventional flow cytometry method.
- Besides the compatibility, Cellometer Vision method also has several advantages over conventional flow cytometry:
  - In comparison to the 300 µL of sample for flow cytometry, only 20 µL of sample is required for the Cellometer Vision. It can immediately provide both concentration and percentage of each cell population, whereas further postharvest analysis is usually required to obtain flow cytometry results and indirect calculation is needed to obtain cell concentration.
  - In addition, the ability to record both BR and FL images of cell sample allows visualization of cell detection and image analysis, which cannot be done by conventional flow cytometry.
  - Also, the counting algorithm enables declustering of clumpy cells, which improves accuracy and consistency of population analysis.
  - Furthermore, the lack of high power lasers or photo-multiplying tubes in the Cellometer systems eliminates the need for precise optical alignment, where the simple epifluorescence setup does not require daily user maintenance.
- Further improvement in instrument sensitivity, counting volume, and higher throughput will make it more versatile in the future.

References

1. Diermeier-Daucher, S., et al., Cell Type Specific Applicability of 5-Ethynyl-2 '-deoxyuridine (EdU) for Dynamic Proliferation Assessment in Flow Cytometry. *Cytometry Part A*, 2009. 75A(6): p. 535-546.
2. Sena, G., et al., Measuring the complexity of cell cycle arrest and killing of drugs: Kinetics of phasespecific effects induced by Taxol. *Cytometry*, 1999. 37(2): p. 113-124.
3. Tao, D.D., et al., New method for the analysis of cell cycle-specific apoptosis. Cytometry Part A, 2004. 57A(2): p. 70-74.
4. Chan, L.L., et al., Direct concentration and viability measurement of yeast in corn mash using a novel imaging cytometry method. *J Ind Microbiol Biotechnol*, 2011. 38(8): p. 1109-15.
5. Pirani, A., Yeast concentration and viability using image-based fluorescence analysis. *Nat Meth*, 2010.
6. Groschel, B. and F. Bushman, Cell cycle arrest in G2/M promotes early steps of infection by human immunodeficiency virus. *J Virol*, 2005. 79(9): p. 5695-704.
7. Poxleitner, M.K., S.C. Dawson, and W.Z. Cande, Cell cycle synchrony in Giardia intestinalis cultures achieved by using nocodazole and aphidicolin. *Eukaryot Cell*, 2008. 7(4): p. 569-74.
8. Chen, G., J. Shu, and D.W. Stacey, Oncogenic transformation potentiates apoptosis, S-phase arrest and stress-kinase activation by etoposide. *Oncogene*, 1997. 15(14): p. 1643-51.

Revvity, Inc.
940 Winter Street
Waltham, MA 02451 USA
www.revvity.com